

Letter

## Crossing of the $\pi d_{5/2}$ and $\pi g_{7/2}$ orbitals in the ${}_{51}\text{Sb}$ isotopes

M.-G. Porquet<sup>1,a</sup>, S. Péru<sup>2</sup>, and M. Girod<sup>2</sup>

<sup>1</sup> CSNSM IN2P3-CNRS and Université Paris-Sud, 91405 Orsay, France

<sup>2</sup> CEA/DIF, DPTA/SPN, BP 12, 91680 Bruyères-le-Châtel, France

Received: 25 February 2005 /

Published online: 7 September 2005 – © Società Italiana di Fisica / Springer-Verlag 2005

Communicated by D. Schwalm

**Abstract.** Self-consistent calculations using the D1S Gogny force have been performed in order to study the mechanism involved in the crossing of the  $\pi d_{5/2}$  and  $\pi g_{7/2}$  orbitals in the Sb isotopes. This inversion is well predicted by the HFB + blocking calculations with spherical symmetry performed for the odd- $A$  Sb isotopes. In addition, several HFB and HF calculations have been performed for even-even nuclei of the five neighbouring isotopic chains ( $Z = 46$  to  $54$ , from the proton dripline to  $N = 82$ ). The results obtained for the binding energies of the two proton orbitals indicate that the radii of the systems play an important role in the crossing, even though some particular  $\pi\nu$  interactions also give a contribution. The spin-orbit interaction, which is known to be concentrated mainly at the nuclear surface, is proposed to be the main responsible of the crossing.

**PACS.** 21.10.Dr Binding energies and masses – 21.60.Ev Collective models – 21.60.Jz Hartree-Fock and random-phase approximations – 27.60.+j  $90 \leq A \leq 149$

### 1 Introduction

The question of the persistence of the magic numbers in the very exotic nuclei is the object of many experimental and theoretical studies at the present time. In the light-mass nuclei, recent results show an evolution of the sub-shell spacings for the nucleons of one type as a function of the filling of particular sub-shells by the other type (see, for instance, [1–3]). As for the very exotic heavy nuclei, the experimental studies need new experimental devices which are not yet available. Meanwhile, experimental results in some nuclei close to stability can be used with benefit, their analysis giving us new tracks which would be helpful when predicting the properties of nuclei very far from the stability valley.

It has been known for a long time that the value of the angular momentum of the ground state of the odd- $A$  antimony nuclei changes as a function of the number of neutrons: it is  $5/2^+$  in the light isotopes and  $7/2^+$  for  $A \geq 123$  [4]. Such a change can be naturally interpreted by the crossing in energy of the two proton orbitals located just above the  $Z = 50$  shell closure, namely  $\pi d_{5/2}$  and  $\pi g_{7/2}$ , when the number of neutrons increases from 70 to 72. The question is then to understand the reason of this inversion.

It was recently suggested [5] that due to strong interactions with particular neutron orbitals, the  $\pi g_{7/2}$  orbital would lower its energy below to that of  $\pi d_{5/2}$  which would be less sensitive. Such an argument had already been put forward a long time ago. The inversion of the two proton orbitals between  ${}^{121}\text{Sb}$  and  ${}^{123}\text{Sb}$  was explained by the “stabilization of the  $\pi g_{7/2}$  state due to the two extra neutrons going into  $h_{11/2}$  orbits which start no later than for 71 neutrons” [6].

From another point of view, *i.e.* the mean-field approach, this crossing can be induced by the increase of the radius of the nucleus with the mass number. This is illustrated in fig. 2-30 of ref. [7] giving the energies of the *neutron orbitals* in a Woods-Saxon (WS) potential as a function of the mass number  $A$ , for nuclei located near the *stability line*. Several crossings in energy of orbitals having various  $\ell$  values can be noticed, successively  $s_{1/2}$  and  $d_{3/2}$  for  $A \sim 60$ ,  $p_{3/2}$  and  $f_{5/2}$  for  $A \sim 95$ ,  $d_{5/2}$  and  $g_{7/2}$  for  $A \sim 135$ ,  $f_{7/2}$  and  $h_{9/2}$  for  $A \sim 180$ . It is worth pointing out that no parameter of the Woods-Saxon potential involves  $\pi\nu$  interactions. Therefore, all these crossings are attributed to the different increases of the separation energies of the orbitals, when the radius of the mean-field potential increases.

To study the mechanism of the crossing known in Sb isotopes, we have performed *self-consistent* calculations

<sup>a</sup> e-mail: porquet@csnsm.in2p3.fr

with the Hartree-Fock-Bogoliubov (HFB) and Hartree-Fock (HF) approaches using the D1S Gogny force. This allows us, at the same time, to take care of the effects due to interactions between nucleons and of those due to the radius of the resulting mean-field potential.

## 2 The $5/2^+$ and $7/2^+$ states in Sb nuclei from the HFB + blocking method

In addition to changes of their ground-state spin, the odd- $A$  antimony nuclei exhibit different excited states. For  $117 \leq A < 123$ , the excitation energy of a  $7/2^+$  state decreases with increasing neutron number, and for  $123 \leq A \leq 133$ , an excited state with spin  $5/2^+$  increases in energy with the neutron number (the measured energies of these states are given in table 1). As discussed in ref. [8], the wave function of the  $7/2^+$  state identified in the light isotopes ( $A \leq 115$ ) is mixed ( $\pi g_{7/2}$  and  $\pi d_{5/2} \otimes 2^+_{\text{core}}$ ), consequently its energy is not pertinent for this study.

We have performed HFB calculations with the Gogny force using the D1S parametrization [9]. All the terms of the Gogny force are included in the present work, in particular the Coulomb exchange and the two-body center-of-mass correction are taken into account. As in ref. [9], the description of an odd- $A$  nucleus is done using the blocking method, imposing that the odd particle is located in one particular orbital chosen by its values of angular momentum and parity. The calculated binding energy of the nucleus is then analyzed as a function of the occupied orbital, that gives the ground state and the excited states. Since the detailed spectroscopic study of all these antimony nuclei (see the discussion in ref. [8]) indicates that the  $5/2^+$  and  $7/2^+$  states are associated to a spherical shape, all the calculations have been performed using the spherical symmetry.

The calculated results (reported in table 1) are in very good agreement with the experimental results:

- i) The ground state of  $^{109-119}\text{Sb}$  is the  $\pi d_{5/2}$  state, and the excited  $\pi g_{7/2}$  state decreases linearly in energy when the number of neutrons increases.
- ii) The ground state of  $^{121-133}\text{Sb}$  is the  $\pi g_{7/2}$  state, and the excited  $\pi d_{5/2}$  state increases linearly in energy with increasing neutron number.

We can notice that the calculated crossing of the two proton orbitals occurs two mass numbers too early, but it is only a matter of about 100 keV.

The energy differences between the  $7/2^+$  state and the  $5/2^+$  state (taken as a reference) of the Sb isotopes are drawn as a function of the mass number in fig. 1. We can clearly see different evolutions of the theoretical results for three groups of masses (109–115, 117–121, and 123–133). The experimental results exhibit the same behaviour, the experimental points ( $A = 117-133$ ) are located along two lines. These changes of slope obviously remind us of the influence of neutron orbitals which are successively filled when the mass number increases from 109 to 133.

While these HFB calculations of Sb isotopes predict the inversion of the two proton orbitals very well, the underlying mechanism cannot be identified from this sole

**Table 1.** Energies (in keV) of the  $5/2^+$  and  $7/2^+$  states of the Sb isotopes with  $A = 109-133$ . The experimental values are from [4, 8].

$A$	$5/2^+$	$7/2^+$	$5/2^+$	$7/2^+$
	$E$ (exp)	$E$ (exp)	$E$ (th)	$E$ (th)
109	0	–	0	944
111	0	–	0	735
113	0	–	0	523
115	0	–	0	338
117	0	527	0	200
119	0	270	0	85
121	0	37	31	0
123	160	0	151	0
125	332	0	276	0
127	491	0	411	0
129	645	0	550	0
131	798	0	692	0
133	962	0	842	0

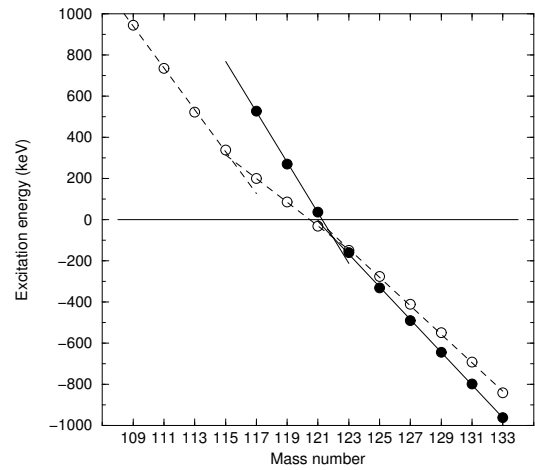


**Fig. 1.** Evolution of the excitation energy of the  $7/2^+$  state relative to the  $5/2^+$  state in the  $^{109-133}\text{Sb}$  isotopes: the experimental results are drawn with full symbols and theoretical results with empty symbols.

result. To have a deeper insight into the inversion we have calculated the binding energies of the proton orbitals in the neighbouring even-even isotopes of five isotopic chains. The results are discussed in the next section.

## 3 Binding energies of the proton orbitals in the neighbouring even-even isotopes

### 3.1 HFB calculations with the Gogny force

The single-particle levels in the neighbouring even-even isotopes have been obtained from HFB calculations. As in ref. [10], the HFB equations are solved by iterative diagonalization of the HFB Hamiltonian, then the single-particle energies are defined as the eigenvalues of the HF part.

In the five isotopic series ( $Z = 46-54$ ), the two proton orbitals,  $\pi d_{5/2}$  and  $\pi g_{7/2}$ , are also found to cross. For each

**Table 2.** Theoretical binding energies ( $BE$  in MeV) of the proton orbitals,  $\pi d_{5/2}$  and  $\pi g_{7/2}$  on each side of the crossing, for the five isotopic series ( $Z = 46$ –54). The parameter  $\bar{R}$  (in fm) is the root-mean-square radius calculated using the matter density stemming from the HFB calculations.

	$N$	$A$	$BE$ ( $\pi d_{5/2}$ )	$BE$ ( $\pi g_{7/2}$ )	$\bar{R}$ (fm)
${}_{46}\text{Pd}$	72	118	-6.473	-6.332	4.640
	74	120	-7.159	-7.174	4.663
${}_{48}\text{Cd}$	72	120	-5.908	-5.866	4.652
	74	122	-6.592	-6.692	4.674
${}_{50}\text{Sn}$	70	120	-4.647	-4.591	4.642
	72	122	-5.349	-5.416	4.665
${}_{52}\text{Te}$	68	120	-3.472	-3.373	4.648
	70	122	-4.181	-4.205	4.672
${}_{54}\text{Xe}$	68	122	-3.024	-3.007	4.679
	70	124	-3.724	-3.822	4.702

isotopic chain, table 2 shows the two masses located on each side of the crossing, the binding energies of the two proton orbitals, and the values of the parameter  $\bar{R}$  (in fm) which is the root-mean-square radius calculated by using the matter density stemming from the corresponding HFB calculations.

Let us stress the fact that the inversion of the two proton orbitals does not take place for identical neutron number, as could be expected if it was due to particular  $\pi\nu$  interactions. On the other hand, the crossing is correlated to the size of the nucleus. By interpolating the results presented in table 2, we can deduce the values of  $\bar{R}$  for which both orbitals in the five isotopic chains have the same binding energy: they are included in a very narrow interval, 4.66–4.68 fm. As a comparison, the value of  $\bar{R}$  varies from 4.64 to 4.73 fm for the five  $N = 72$  isotones ( $Z = 46$ –54). These results motivate our explanation of crossing of the two proton orbitals by the size effect.

As an illustration, fig. 2 shows the HFB results for Sn isotopes. The binding energies of the two proton orbitals exhibit no large trend deviation, meaning that there is no sign of strong  $\pi\nu$  interactions. Both energies decrease as a function of the neutron number, the slope corresponding to the  $\pi g_{7/2}$  orbital being slightly larger over the whole mass interval.

Three linear portions ( $58 < N < 64$ ,  $66 < N < 70$ , and  $72 < N < 82$ ) can be identified (see fig. 2). These ranges are found to remain the same in the five isotopic series. It is worth pointing out that, as mentioned above (see sect. 2), the results of the Sb calculations give the same ranges. The changes of slope can be connected with the filling of the neutron sub-shells. Therefore, we analyzed the values of the occupation probability of the different neutron orbitals calculated by HFB. Because of the pairing correlations, it is very difficult to correlate the occupation probabilities of the sub-shells with the neutron numbers where the slope is changing. For example at the first break ( $N = 64$ –66), the  $\nu g_{7/2}$  sub-shell is still not

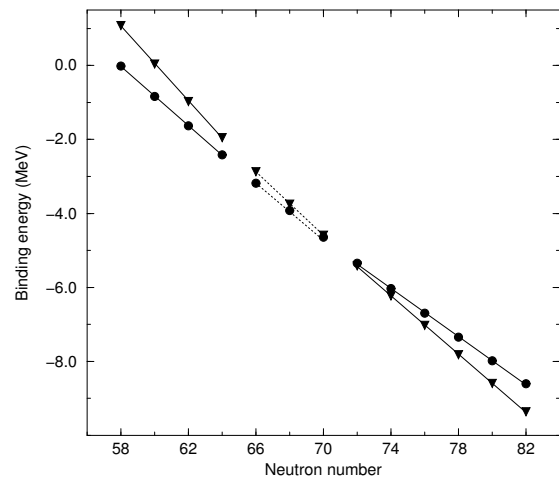


**Fig. 2.** Binding energies of the  $\pi d_{5/2}$  (circle) and  $\pi g_{7/2}$  (tri-angle down) orbitals in the  ${}^{108-132}\text{Sn}$  isotopes, from HFB self-consistent calculations using the D1S effective force of Gogny.

full (occupation probability  $v^2 \sim 0.75$ ), the  $\nu s_{1/2}$  sub-shell is half-filled, the  $\nu d_{3/2}$  and the  $\nu h_{11/2}$  sub-shells start to be filled ( $v^2 \sim 0.30$  and  $0.15$ , respectively). To precisely study the influence of each neutron sub-shell on the slope of the binding energies of the two relevant proton orbitals, Hartree-Fock calculations (without pairing) have been performed.

### 3.2 HF calculations with the Gogny force

The single-particle levels in the five isotopic series have been obtained from HF calculations. As usual, the HF equations are solved by iterative diagonalization of the HF Hamiltonian. Then the single-particle energies are defined as the eigenvalues of the self-consistent one-body Hamiltonian, obtained after convergence.

The binding energies of the two proton orbitals are more closely correlated with the neutron active orbital than for previous HFB calculations. As an example, the Sn results are displayed in fig. 3. The  $\pi g_{7/2}$  orbital crosses the  $\pi d_{5/2}$  orbital between  $N = 62$  and  $N = 64$  (when  $\nu g_{7/2}$  is full). Then, when  $\nu s_{1/2}$  starts to fill, the order changes again. The second inversion takes place between  $N = 72$  and  $N = 74$  (when  $\nu h_{11/2}$  starts to fill).

For each of the isotopic series, we can group the points according to three lines having very different slopes: i) the first one corresponds to  $N = 58$ –64 (filling of  $\nu g_{7/2}$ ); ii) the second,  $N = 66$ –70 (filling of  $\nu s_{1/2}$  and  $\nu d_{3/2}$ ); iii) the third,  $N = 72$ –82 (filling of  $\nu h_{11/2}$ ). The results of these linear fits are reported in table 3. First of all, we can notice that the very large value of the slope of the  $\pi g_{7/2}$  binding energy occurs for the filling of the neutron sub-shell with the same angular momentum ( $\nu g_{7/2}$ ). It is almost twice as large as that of the  $\pi d_{5/2}$  orbital. That leads to the first inversion between  $N = 62$  and  $N = 64$  (see fig. 3). For the other neutron sub-shells, slope values for both proton orbitals are of the same order. More precisely, those

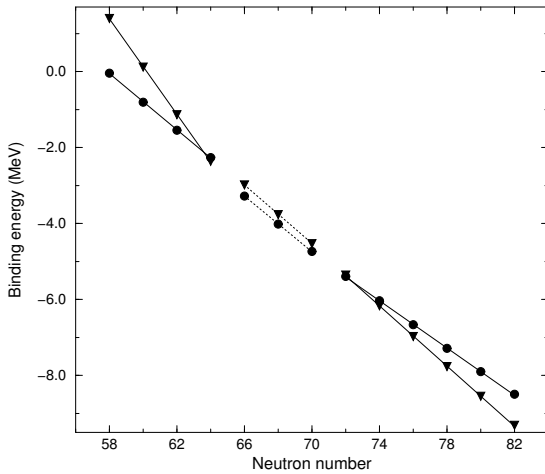


**Fig. 3.** Binding energies of the  $\pi d_{5/2}$  (circle) and  $\pi g_{7/2}$  (triangle down) orbitals in the  $^{108-132}\text{Sn}$  isotopes, from HF self-consistent calculations using the D1S effective force of Gogny.

**Table 3.** Slope values (keV/ $N$ ) of the three linear parts of the  $\pi d_{5/2}$  and  $\pi g_{7/2}$  binding energies obtained from HF calculations using the Gogny force. The values corresponding to the  $\pi d_{5/2}$  orbital are written in *italic* and the ones corresponding to the  $\pi g_{7/2}$  orbital are written in **bold**.

Filling of	$\nu g_{7/2}$ ( $N = 58-64$ )		$\nu s_{1/2}/d_{3/2}$ ( $N = 66-70$ )		$\nu h_{11/2}$ ( $N = 72-82$ )	
	$_{48}\text{Cd}$	<i>-374</i>	<b>-631</b>	<i>-369</i>	<b>-389</b>	<i>-315</i>
$_{50}\text{Sn}$	<i>-371</i>	<b>-627</b>	<i>-366</i>	<b>-385</b>	<i>-311</i>	<b>-393</b>
$_{52}\text{Te}$	<i>-355</i>	<b>-630</b>	<i>-363</i>	<b>-384</b>	<i>-305</i>	<b>-389</b>
$_{54}\text{Xe}$	<i>-340</i>	<b>-633</b>	<i>-360</i>	<b>-383</b>	<i>-294</i>	<b>-385</b>

corresponding to the  $\pi g_{7/2}$  orbital are always slightly larger, irrelevant of the neutron active sub-shells.

In this calculation performed without pairing correlations, we clearly observe the expected effect of the neutron sub-shells fillings. In that particular case, the heavy nuclei behave the same as the light nuclei: the occupation of some sub-shells by one type of nucleons has a crucial effect on the energy of the sub-shells of the other type.

## 4 Discussion

The first inversion obtained in the HF calculations between  $N = 62$  and  $N = 64$  vanishes in the HFB calculations because it is not robust enough. The crossing happens for larger  $N$ , since the binding energy of the  $\pi g_{7/2}$  orbital always decreases faster than that of the  $\pi d_{5/2}$  orbital. The steeper slope of the binding energy of the  $\pi g_{7/2}$  orbital is attributed at the same time, to its larger  $\ell$  value, and to its interactions with the neutron sub-shells, particularly the  $\nu g_{7/2}$  sub-shell and, to some extent, the  $\nu h_{11/2}$  sub-shell. It is worth pointing out that, because of the pairing correlations, all these  $\pi\nu$  interactions are spread on a very large mass interval.

Finally, the energies of the proton orbitals have been obtained by solving the Schrödinger equation with a

Woods-Saxon average potential. Using the “universal” parameters [11,12], the  $\pi d_{5/2}$ - $\pi g_{7/2}$  inversion is observed, but occurs at  $A \sim 132$ , *i.e.* ten mass numbers away from the experimental inversion. The location of the inversion strongly depends on the WS parameter values, for instance Chepurnov’s parametrization [13] does not lead to any inversion, whereas Rost’s values [14] give the inversion at  $A \sim 120$ . Since the parametrizations (strength and radius parameters) of the spin-orbit part of these three sets are very different (see refs. [12–14]), one can conclude that the crossing of the two proton orbitals is mainly driven by the spin-orbit part of the WS potential.

In order to challenge this proposition, we have performed HFB calculations of the Sn isotopes, varying the strength of the two-body spin-orbit interaction of the D1S Gogny force by 15%. While the crossing occurs at  $A = 121$  (see table 2) when using the standard value  $W_{\text{SO}} = -130$  MeV, it is calculated at  $A = 108$  for  $W_{\text{SO}} = -110$  MeV and  $A = 128$  for  $W_{\text{SO}} = -150$  MeV. Such a result can be easily understood. The  $\pi g_{7/2}$  orbital is the higher-lying member of a spin-orbit doublet, while the  $\pi d_{5/2}$  orbital is a lower-lying one, so that their energy difference strongly depends on the strength of the spin-orbit interaction. Moreover, their energy variations as a function of the neutron number are closely connected with the radius of the nuclear potential because the spin-orbit interaction is concentrated mainly at the nuclear surface.

## 5 Conclusion

The increase of the nuclear radii does not lead to a uniform compression of the energy eigenvalues of the average potential. The energy decrease depends on the angular momentum of the orbital. We have shown that the inversion of the  $\pi d_{5/2}$  and  $\pi g_{7/2}$  orbitals, deduced from the change of the Sb ground-state spin value, is very well predicted by HFB + blocking calculations using the Gogny force D1S. Several calculations performed in the neighbouring even-even isotopes allowed us to study the influence of the radius increase as well as that of the  $\pi\nu$  interactions. Moreover, the spin-orbit part of the interaction, which is known to be peaked at the nuclear surface, is proposed to be the main responsible of the crossing of these two proton orbitals.

For every major shell  $N$ , an inversion of eigenstates associated to a spherical shape could be foreseen. The radius of the system exists at which the orbital with  $\ell = N - 2$  ( $j = \ell + 1/2$ ) crosses the orbital with  $\ell = N$  ( $j = \ell - 1/2$ ). Nevertheless, the *direct observation* of such a crossing is not common. For the above radius values, i) the Fermi level has to be close to crossing orbitals, and ii) the corresponding nuclei have to be spherical, in order to ensure that an observed crossing does not result from a possible change of deformation. The isotopic chain of Sb nuclei fulfills all the above conditions. Other cases are under consideration.

We are grateful to Dr E. Bauge and Dr R. Lucas for their careful reading of the manuscript.

## References

1. Y. Utsuno *et al.*, Phys. Rev. C **60**, 054315 (1999).
2. A. Ozawa *et al.*, Phys. Rev. Lett. **84**, 5493 (2000).
3. T. Otsuka *et al.*, Phys. Rev. Lett. **87**, 082502 (2001).
4. R.B. Firestone (Editor), *Table of Isotopes*, 8th edition (Wiley, New York, 1996).
5. R.F. Casten, *Nuclear Structure from A Simple Perspective*, 2nd edition (Oxford University Press, 2000).
6. A. de-Shalit, M. Goldhaber, Phys. Rev. **92**, 1211 (1953).
7. A. Bohr, B. Mottelson, *Nuclear Structure*, Vol. **1** (Benjamin, New York, 1969).
8. M.-G. Porquet *et al.*, Eur. Phys. J. A **24**, 39 (2005).
9. J. Dechargé, D. Gogny, Phys. Rev. C **21**, 1568 (1980); J.-F. Berger, M. Girod, D. Gogny, Comput. Phys. Commun. **63**, 365 (1991).
10. S. Péru, M. Girod, J.-F. Berger, Eur. Phys. J. A **9**, 35 (2000).
11. R. Bengtsson, J. Dudek, W. Nazarewicz, P. Olanders, Phys. Scr. **39**, 196 (1989).
12. J. Dudek, Z. Szymanski, T. Werner, Phys. Rev. C **23**, 920 (1981).
13. V.A. Cherpunov, Sov. J. Nucl. Phys. **6**, 696 (1968).
14. E. Rost, Phys. Lett. B **26**, 184 (1968).